

## CHEMICAL AND STRUCTURAL MODIFICATIONS INDUCED IN STRUCTURAL MATERIALS BY ELECTROCHEMICAL PROCESSES

V. ANDREI<sup>1</sup>, GH. VLAICU<sup>2</sup>, M. FULGER<sup>1</sup>, C. DUCU<sup>3</sup>, C. DIACONU<sup>1</sup>, GH. ONCIOIU<sup>1</sup>,  
E. ANDREI<sup>1</sup>, M. BAHRIM<sup>4</sup>, A. GHEBOIANU<sup>2</sup>

<sup>1</sup>*Institute for Nuclear Research, 115400, Mioveni, Arges, Romania, E-mail: anvdic12@yahoo.com*

<sup>2</sup>*“Valahia” University of Târgoviște, Physics Department, 130024, Târgoviște, Romania,  
gvlaicu@yahoo.com*

<sup>3</sup>*Research Center for Advanced Materials, University of Pitești, Romania*

<sup>4</sup>*High School of Constanța, Romania*

(Received October 9, 2008)

*Abstract.* The surface properties of carbon steel SA 106, austenitic stainless steel 304 and martensitic stainless steel 403 was modified by thermo-electrochemical nitrating and carburizing treatments using plasma electrolytic processes, to improve the corrosion behavior. The surfaces films developed by surface treatments were investigated by optical microscopy, XPS, XRD and EIS. Corrosion behavior was evaluated by electrochemical techniques. The paper gives an overall description of various aspects concerning structures and properties developed by surface electrochemical treatments.

*Key words:* XPS, XRD, EIS, surface films.

### 1. INTRODUCTION

Recently, surface electrochemical engineering processes which modify the surfaces of engineering components to improve their in-service performance, useful working lifetimes, aesthetic appearance or economics of production, have attracted a lot of interest [1,2]. The purpose may be to reduce corrosion, reduce frictional energy losses, reduce wear, act as a diffusion barrier, provide thermal insulation, exclude certain wavelengths of radiation, promote radiation electronic interactions, electrically insulate or simply improve the aesthetic appearance for the surface. Plasma Electrolysis (PE) is a generic term which is used to describe a variety of high voltage electrochemical processes, which feature plasma-discharge phenomena occurring at an electrode-electrolyte interface [2]. Extensive trials were carried out in order to develop nitrating and nitro-carburizing plasma electrolytic diffusion treatments for a group of materials, including Al, Ti, and stainless steels. However, major uncertainties remained concerning the process optimization,

control and repeatability, which were mainly caused by the fact that the scientific understanding of key process fundamentals and discharge phenomena lagged well behind empirically based treatment trials then in progress. A first step towards closing these knowledge gap between fundamental process understanding and coating characteristics is the characterization of the non-homogeneous surface structures developed by plasma-assisted electrochemical processes.

In this paper the results of the characterization of surface structures developed on some structural nuclear materials, by surface electrochemical treatment methods for improvement of the properties (corrosion resistance, hardness, wear properties) are reported.

## 2. EXPERIMENTAL

Thermo-electrochemical treatments of carburizing and nitrating bath were applied using the equipment TEC100 (SCINTI – Chisinau) on carbon steel SA 106, austenitic steel 304 and martensitic steel 403. The experimental setup was identically for carburizing (using glycerine solution as electrolyte) and nitrating (using  $\text{NH}_4\text{OH}$  solution as electrolyte) treatments.

The parameters of the thermo-electrochemical treatments are presented in the Table 1.

The surfaces films developed by surface treatments were investigated by optical microscopy, ESCA, XRD and electrochemical impedance spectroscopy. Corrosion behavior was evaluated by electrochemical techniques.

Optical measurements were performed with NEOPHOT 2 optical microscope, and the microstructures of the treated materials were studied.

ESCA analysis (X-ray Photoelectron Spectroscopy-XPS) of the deposited films have been performed with an ESCALAB MK II (V.G.Scientific) spectrometer. The residual pressure inside the measurement chamber was  $10^{-9}$  Torr.

The X-ray Al  $K\alpha$  ( $E=1486.6$  eV) radiation was used and the calibration of the instrument was obtained taking as reference the silver line Ag 3d 5/2 at 368.2 eV.

The X-ray diffraction data of austenitic steel 304 and martensitic steel 403 were collected at room temperature. Data acquisitions were made with a DRON UM1 diffractometer connected with PC. A horizontal powder goniometer in Bragg-Brentano focusing geometry with graphite monochromator was used. The incident Cu- $K\alpha$  line, at 36 kV and 30 mA was used. The typical experimental conditions were: 10s for each step, range angle  $2\theta = 25-120^\circ$ , with a step of  $0.05^\circ$ . The patterns obtained in these conditions were used to make qualitative phase analysis. The range angle  $2\theta = 34-46^\circ$  containing the 100% intensity peaks of  $\text{Fe}_3\text{O}_4$ ,  $\text{Fe}_{15}\text{Cr}_4\text{Ni}_2$ ,  $(\text{Cr,Fe})_7\text{C}_3$ , CrN, FeO, CrC and CrFe were measured with a better statistics, 20s for each step. In the same angular range the low angle incidence diffraction in order to determine the phase's presence in the surface films [3, 4] from 1.0 to 8.0  $^\circ$  incidence angle was performed.

Table 1

## Thermo-electrochemical treatment (TE)

Material	TE	Sample code	Experimental parameters
Carbon steel SA 106	Carburizing	106_C	$U=220V, I=6A, t=3min$
	Nitrating	106_N	$U=165V, t=3min$
Austenitic steel 304	Carburizing	304_C	$U=220V, I=6A, t=3min$
	Nitrating	304_N	$U=165V, t=3min$
Martensitic steel 403	Carburizing	403_C	$U=220V, I=6A, t=3min$
	Nitrating	403_N	$U=165V, t=3min$

Electrochemical impedance spectroscopy (EIS) measurements were performed using an Princeton Applied Research 273 System (Potentiostat/ Galvanostat), with Model 5210 Lock-in Amplifier.

To characterize the oxide layers developed on the steels surface (304 and 403) the EIS measurements were performed at the open circuit potential, because at this value which correspond of the very small current into oxide layer, the thickness of this oxide is not modified.

The solution used in tests was the boric acid/ borax because that is a chemical inert environment for the superficial films developed on the samples.

### 3. RESULTS

The results about the microstructures of treated samples and about corrosion rates (determined by polarization resistance method) are presented in the Table 2.

From EIS method we can obtain qualitative information (from Bode and Nyquist plots analysis) and quantitative information from equivalent circuit models which are commonly used to interpret impedance data.

Table 2

## Microstructure of the films and corrosion rate

Sample	Surface film structure	Corrosion rate (mm/y)
106_C	Surface film -10 $\mu$	$1.9 \times 10^{-6}$
106_N	Stratification surface structure: Compound layer-100 $\mu$ Diffusion layer -100 $\mu$	$2 \times 10^{-6}$
SA 106 as received		$2.03 \times 10^{-6}$
304_C	Surface film -50 $\mu$	$0.07 \times 10^{-6}$
304_N	Surface film -10 $\mu$	$1.14 \times 10^{-6}$
304 as received		$2 \times 10^{-6}$
403-C	Surface film - 400 $\mu$	$0.3 \times 10^{-6}$
403-N	Surface film - 150 $\mu$	$0.6 \times 10^{-6}$
403 as received		$2.2 \times 10^{-6}$

In the case of carburized and nitrating 304 samples the highest impedance values are closed to  $105\Omega$ .

The angle phases are smaller than 90 degree that signifies that films are not fully capacitive. For carburized 304 sample the angle phase has a greater value (63 degree) than nitrating 304 sample (48 degree) so, the films obtained by carburization are less porous.

The films capacitances calculated from equivalent circuit models can give some information. So, smaller values of the capacitances correspond to a slow growth of the layers indicating a stability of this passive layer. The very high values of electrical resistances demonstrate a good corrosion resistance. The following values  $C_{\text{layer}} = 6.244 \times 10^{-5} \text{ F/cm}^2$  and  $R_{\text{layer}} = 1.9 \times 10^4 \Omega\text{cm}^2$  for carburized 304, and  $C_{\text{layer}} = 1.065 \times 10^{-4} \text{ F/cm}^2$ ;  $R_{\text{layer}} = 5.836 \times 10^4 \Omega\text{cm}^2$  for nitrating 304 denote that the layer obtained by carburization is thicker, corrosion resistant and protective.

From Nyquist plot were obtained the values of polarization resistances. The value of polarization resistance for carburized sample is  $70,000\Omega\text{cm}^2$  and for nitrating sample  $33,000\Omega\text{cm}^2$ ; a greater polarization resistance indicate a smaller corrosion rate.

The impedance value for carburized 403 is greater than  $106 \Omega$  and greater than the impedance value of the nitrating 403 ( $Z > 104 \Omega$ ) so the film obtained by cementation has better properties. In both cases the angle phases have values smaller than 900 so the films are not fully capacitive that signify a porosity of films or a roughness of metal surfaces. The angle phase of carburized 403 (48 degree) is greater than the angle phase of nitrating 403 sample (40 degree) so the oxide layer developed by carburizing TE is less porous.

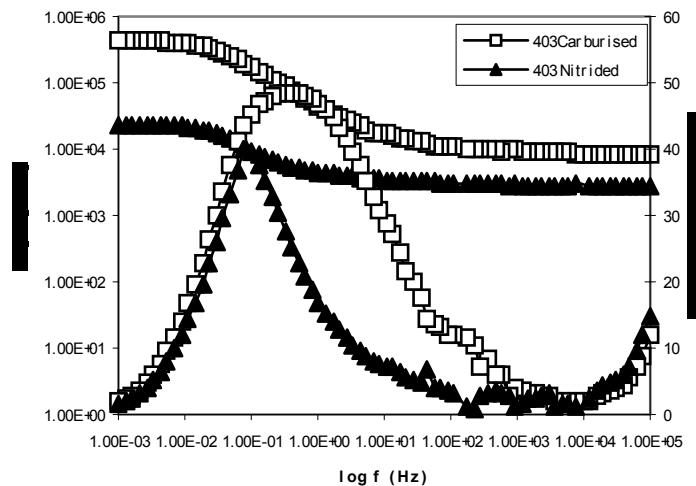


Fig. 1 – Comparative Bode and angle phase plots for 403 carburized and 403 nitrating samples.

The polarization resistance is the diameter of the semicircle which can be found on Nyquist plot real axis value. Polarization resistance for carburized 403 has a great value of  $450 \text{ k}\Omega\text{cm}^2$  comparatively with  $20 \text{ k}\Omega\text{cm}^2$  of nitrating sample and that signifies a very small corrosion rate for carburized sample. In the case of carburized sample the film capacitor acts like a constant phase element (is a non-ideal capacitor because of the non-homogeneous surface) and has a value of  $7.723 \times 10^{-6} \text{ F/cm}^2$ . The value of the film capacitance in the case of nitrating sample is of  $1.64 \times 10^{-4} \text{ F/cm}^2$  which is two magnitude orders greater than carburized sample. A smaller value of coating capacitance signifies an adherent film so, by TE-carburizing treatment can obtain thicker oxide layers.

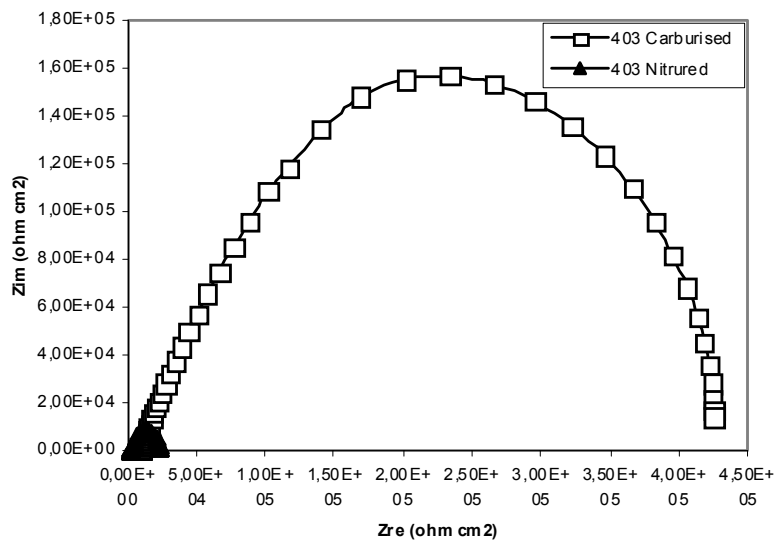


Fig. 2 – Nyquist plot for carburized and nitrating 403 samples.

The very high resistance of carburized 403 sample ( $4,800 \text{ }\Omega\text{cm}^2$ ) implies a good corrosion resistance, i.e. a low corrosion rate.

Figures 3 and 4 show the XRD patterns of the austenitic steel 304 respectively martensitic steel 403 measured at room temperature, in three metallurgical states: as-received, after carburizing and after nitrating treatments.

Figures 5, 6, 7 and 8 show the low angle X-ray diffraction patterns of austenitic and martensitic steel after carburizing and nitrating treatments, acquired between 10 and 80 incidence diffraction angles.

XPS spectra on the austenitic steel 304 and martensitic steel 403 after carburizing and nitrating treatments were recorded and the data quantification was performed using sensitivity factors method [5, 6].

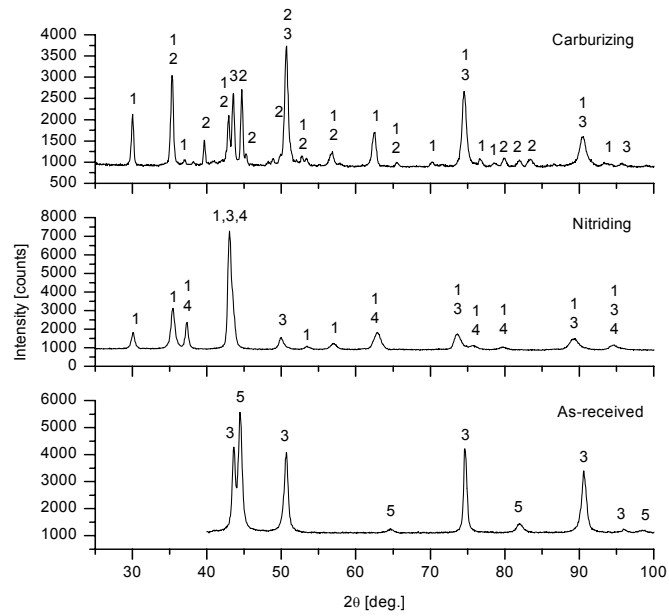


Fig. 3 – XRD patterns of austenitic steel: 1= $\text{Fe}_3\text{O}_4$ , 2= $(\text{Cr,Fe})_7\text{C}_3$ , 3= $\text{Fe}_{15}\text{Cr}_4\text{Ni}_2$ , 4= $\text{CrN}$ , 5= $\text{CrFe}$ .

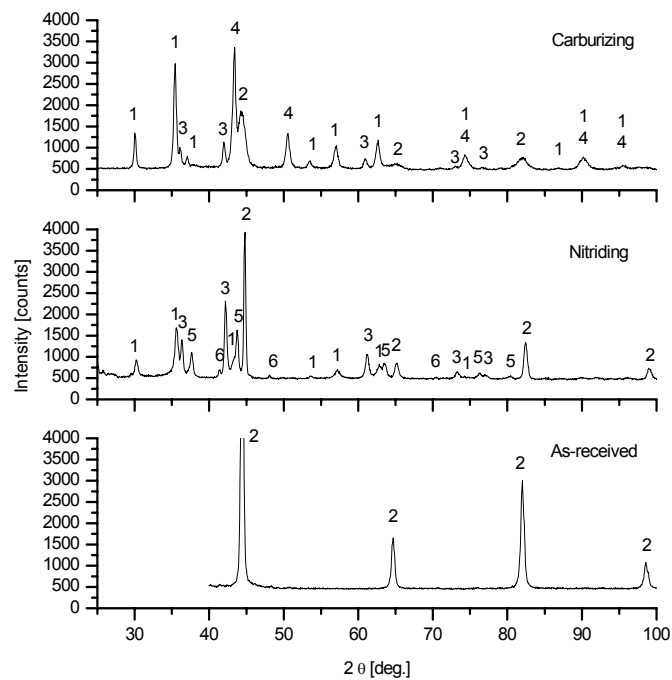


Fig. 4 – XRD patterns of martensitic steel: 1= $\text{Fe}_3\text{O}_4$ , 2= $\text{CrFe}$ , 3= $\text{FeO}$ , 4= $\text{CrC}$ , 5= $\text{CrN}$ , 6= $\gamma\text{Fe}_4\text{N}$ .

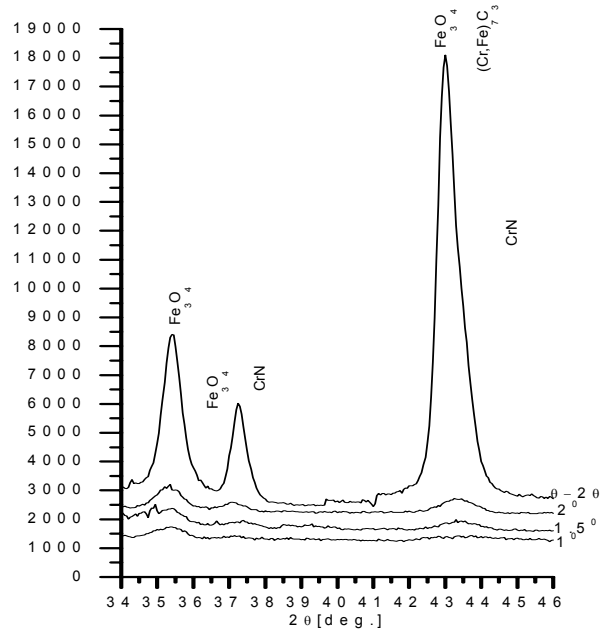


Fig. 5 – LAXRD patterns of austenitic steel 304 after steel 304 carburizing treatment.

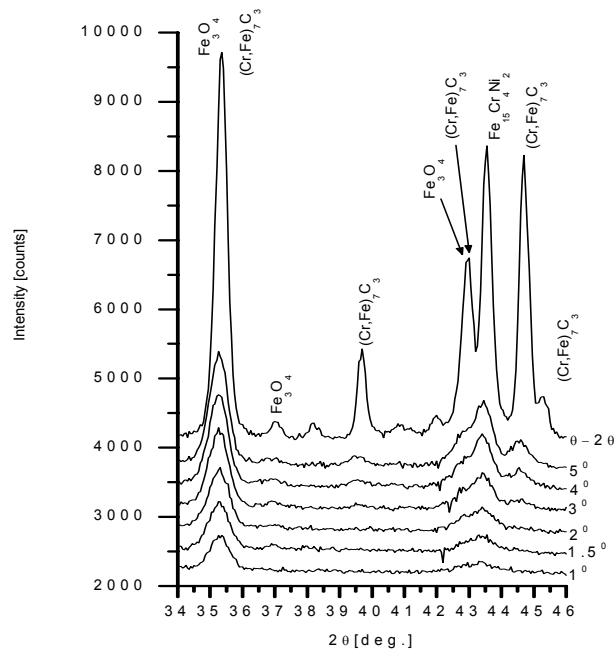


Fig. 6 – LAXRD patterns of austenitic steel 304 after nitriding treatment.

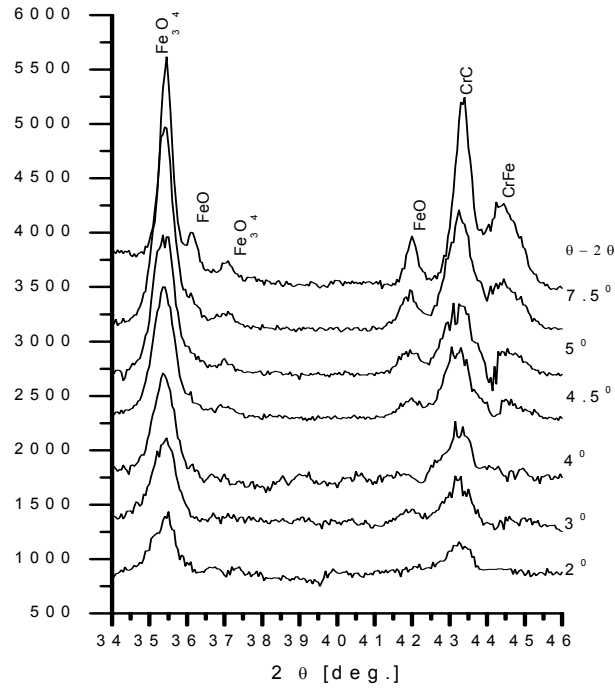


Fig. 7 – LAXRD patterns of martensitic steel 403 after carburizing treatment.

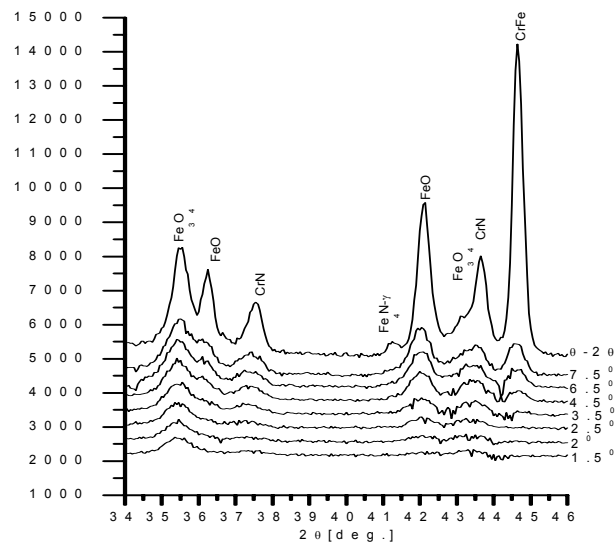


Fig. 8 – LAXRD patterns of martensitic steel 403 after nitriding treatment.

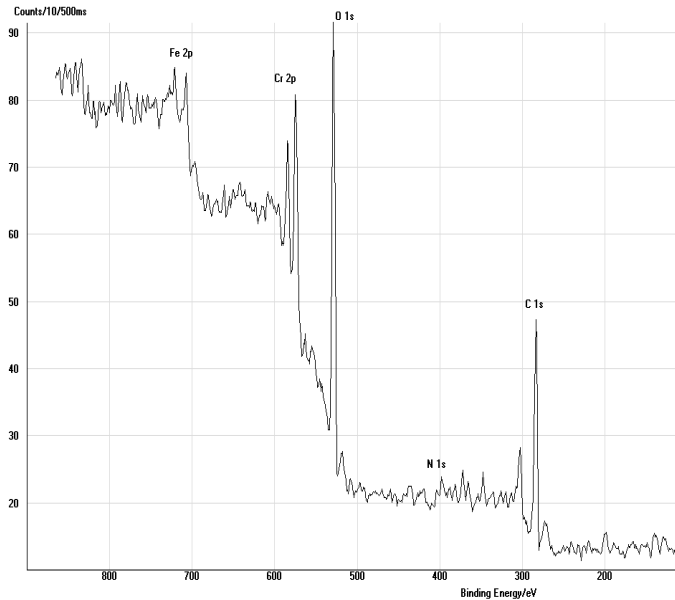


Fig. 9 – Survey XPS spectrum on 304\_C sample.

The surface elemental composition (atomic %) are presented in the Table 3.

Table 3

The surface elemental composition (atomic %)

Sample	304-C	304-N	403-C	403-N
C1S	82.08	68.14	87.58	63.17
FE2P3	1.12	1.8	1.75	0.7
O1S	7.01	7.01	3.84	20.96
NI2P3	0	1.25	0.38	0.16
CR2P	9.79	16.59	6.45	8.61
N1S		5.2		6.4

#### 4. CONCLUSIONS

The carbon steel SA 106, the austenitic steel 304 and the martensitic steel 403 have a very good corrosion behavior, after thermo-electrochemical treatments. The protective oxide layer of  $\text{Fe}_3\text{O}_4$  is growth on austenitic and martensitic steels by thermo electrochemical treatments of carburizing and nitrating. By LAXRD we found that  $\text{Fe}_3\text{O}_4$  appear as external layer both on austenitic and martensitic steel. On to the martensitic steel the surface layer contains also CrC and CrN for carburizing respectively nitrating treatment.

The surface layer microstructures do not differ too much for austenitic and martensitic steel after carburizing treatments. By nitrating treatments, the microstructures of martensitic steel layer is different of austenitic steel surface layer.

For carburizing treatments, the thickness of oxide surface layer on martensitic steel ( $\alpha_{\text{lim}} \approx 4.5^0$ ) is greater than on austenitic steel ( $\alpha_{\text{lim}} \approx 1.5^0$ ). For nitrating treatments, these thicknesses are the same for both steel types ( $\alpha_{\text{lim}} \approx 1.5^0$ ).

### REFERENCES

1. V.I. Ganchar, I.M. Zgardan, A.I. Dicusar, *Surface Engineering and Applied Electrochemistry*, **5**, pp. 13–19 1996.
2. A. Matthews, A. Leyland, A. Yerokhin, T. Pilkington, IGR Report: EPSRC Grant No.GR/ R15696.
3. A. Andrei, G. Vlaicu, C. Ducu, *Characterization of Surface Structures developed on nuclear materials by ESCA and complementary techniques*, Rom. Journ. Phys, **48**, 1–4, 439–445 (2003).
4. C. Ducu, V. Malinovschi, A. Andrei, Microstructures characterization of protective surfaces of nuclear steels, EPDIC-10, Geneva, 2006.
5. D. Briggs, M.P. Seah (eds.), *Practical Surface Analysis*, 2<sup>nd</sup> ed. Vol. I (“Auger and X-ray Photoelectron Spectroscopy”), Wiley, New York, 1990.
6. G. Vlaicu, N. Pavel, F. Parsan, C. Stih, G. Dima, *Comparative study concerning the X-rays fluorescence analysis of the press molten slug samples*, Revista de Chimie, **58**, 11, 1154–1155 (2007).